J.L. Linsky • V.V. Izmodenov • E. Möbius •
R. von Steiger
Editors

From the Outer Heliosphere to the Local Bubble

Comparison of New Observations with Theory

Previously published in *Space Science Reviews* Volume 143,
Issues 1–4, 2009

Springer

J.L. Linsky
JILA, University of Colorado and NIST
Boulder, CO, USA

V.V. Izmodenov
Department of Aeromechanics and
Gas Dynamics
Lomonosov Moscow State University
Moscow, Russia

E. Möbius
Space Science Center and
Department of Physics
University of New Hampshire
Durham, NH, USA

R. von Steiger
International Space Science Institute
Bern, Switzerland

Cover illustration: The cover illustration is a schematic view extending from the heliosphere via the Local Bubble to the Loop I Superbubble on an approximate logarithmic distance scale. The heliosphere—shown with its boundary structures, the solar wind termination shock (TS) and the heliopause (HP)—is moving at ≈26 km/s through a region that may be a transition between the Local Interstellar Cloud (LIC) and the so-called G-Cloud. The outward trajectories and current positions of the most distant spacecraft, the two Voyagers (V1 and V2), are also indicated. Also shown schematically are other interstellar clouds and astrospheres (analogs of the heliosphere around other stars).

Illustration by K. Donahue, J. Linsky, and E. Möbius, adapted from Fig. 1 of "From the Heliosphere to the Local Bubble—What Have We Learned?" by E. Möbius, this volume

Library of Congress Control Number: 2009925997

DOI: 10.1007/978-1-4419-0247-4

ISBN-978-1-4419-0246-7 e-ISBN-978-1-4419-0247-4

Printed on acid-free paper.

1

springer.com

Contents

SECTION III: HOW ARE THE ISM INSIDE AND OUTSIDE OF THE HELIOSPHERE RELATED?

SECTION IV: WHAT ARE THE ENERGY AND PRESSURE BALANCES IN THE LOCAL BUBBLE?

SECTION V: WHAT PHYSICAL PROCESSES DRIVE THE MULTIPHASE INTERSTELLAR MEDIUM IN THE LOCAL BUBBLE?

Group Photograph

Front row, left to right:

Vladimir Baranov
Elena Provornikova
Burkhard Fuchs
Vladimir Florinski
Merav Opher
Hans-Reinhard Müller
André Balogh
Steve Snowden
George Gloeckler
Robin Sheldon
Johannes Geiss
Steve Spangler
Ed Stone
Jonathan Slavin
Nick Pogorelov
Dimitra Koutroumpa
Barry Welsh
Eric Quémerais
Brian Wood
Maciej Bzowski

Back row, left to right:

Eberhard Möbius
Vlad Izmodenov
Alex Lazarian
Ed Jenkins
Jeff Linsky
John Richardson
Dave McComas
Rosine Lallement
Seth Redfield
Rudolf von Steige
Randy Jokipii

Foreword

Jeffrey Linsky · Vlad Izmodenov · Eberhard Möbius

Originally published in the journal Space Science Reviews, Volume 143, Nos 1–4, 1–3.
DOI: 10.1007/s11214-008-9426-0

For many years, studies of the outer heliosphere and the interstellar medium were two interesting research fields developing in near isolation from each other. Theoreticians knew that interstellar gas pressure provides the outer boundary condition for models of the solar wind, but little was known about the properties of interstellar gas either inside or outside of the heliosphere. There were no *in situ* plasma measurements of the distant solar wind to guide their studies of the outer heliosphere and beyond.

Since the 1980s, this situation has changed dramatically as a consequence of several developments: (i) measurements of pickup ions of the interstellar gas flowing through the heliosphere and direct observations of the neutral helium flow, (ii) first the prediction (in 1991) and then the detection (in 1996) of the hydrogen wall in the heliopause, (iii) the development of kinetic-fluid and multifluid theoretical models of the interaction of the solar wind with interstellar plasma including charge exchange, (iv) studies of local interstellar gas using ultraviolet absorption-line spectroscopy of nearby stars, and (v) plasma and magnetic-field measurements from Voyagers 1 and 2 as they crossed the termination shock. These developments have enriched both research fields enormously and demonstrated their inherent interrelations.

The primary drivers for this abrupt change in our understanding of the outer heliosphere and local interstellar medium (LISM) are the critical data provided by space missions. Launched in 1984, the Active Magnetospheric Particle Tracer Explorer Ion Release Module (AMPTE IRM) carried the SUprathermaL Energy Ionic Charge Analyzer (SULEICA) experiment that enabled the discovery of the interstellar pickup ions. Beginning in 1990 and still operating successfully, Ulysses carries the Solar Wind Ion Composition Experiment (SWICS) instrument that measures elemental charge states and composition in the solar wind and the pickup ions that result from the charge exchange of solar wind protons and ions with incoming neutrals. The Hubble Space Telescope (HST), also launched in 1990, initially carried the Goddard High Resolution Spectrometer (GHRS) and since 1997, the

J. Linsky (✉) · V. Izmodenov · E. Möbius
Boulder, CO 80309-0440, USA
e-mail: jlinsky@jila.colorado.edu

Space Telescope Imaging Spectrograph (STIS). Both instruments have measured absorption lines of hydrogen and other elements in the LISM. The Solar and Heliospheric Observatory (SoHO), launched in 1995 and still operating successfully, carries many instruments, including the Solar Wind Anisotropies (SWAN) instrument that measures backscattered-solar Lyman-α radiation that traces the flow of neutral hydrogen in the heliosphere. The Advanced Composition Explorer (ACE), launched in 1997, continues to provide information on solar wind composition and pickup ions. And, we must not forget the intrepid Voyager spacecraft, launched in 1977, that are providing unique information on the plasma and magnetic fields on both sides of the termination shock.

George Gloeckler, to whom this volume is dedicated on the occasion of his seventieth birthday, played a major role in the analysis of data from these space experiments and in our understanding of physical processes in the outer heliosphere and LISM.

The convenors of this ISSI workshop desired a format that would summarize these developments, identify and critically assess the important physical processes, and foster interdisciplinary research. Our specific objectives were to:

– Cross-fertilize the two scientific disciplines by bringing together active researchers with wide expertise in both fields in a setting that provides opportunities for detailed interactions in both the scientific sessions and in informal small groups.
– Discuss the rapidly advancing developments in both theory and observations, mainly due to space experiments.
– Exploit the rich archive of calibrated data and sophisticated theories tested by comparison with observations of nearby interacting plasmas to develop physical insights and models that could be applied to understanding plasma interactions elsewhere in the universe where the data are sparse and compromised by line of sight averages and the theories are less mature and tested.
– Stimulate modelers to test the accuracy of their various numerical codes by computing models with the same input parameters.
– Stimulate the development of broader perspectives.

With these objectives in mind, the convenors formulated a workshop program based on seven questions that the speakers were asked to address:

– What are the dominant physical processes in the termination shock and inner heliosheath?
– What are the three-dimensional shape and structure of the dynamic heliosphere?
– How are the interstellar plasmas and dust located inside and outside of the heliosphere related?
– What are the origin and physical properties of the very local ISM?
– What are the energy and pressure equilibria in the Local Bubble?
– What are the important physical processes in the multiphase interstellar medium located inside the Local Bubble?
– What are the roles that magnetic fields play in the outer heliosphere and Local Bubble?

During the course of the meeting, it became clear that magnetic fields play important roles in most of the phenomena discussed at the workshop. Therefore, the final question may be the most basic of the seven questions to answer.

To place these questions into a broader context, the convenors requested that several speakers give "big picture" talks on the time evolution of the heliosphere, the origin and evolution of the Local Bubble, the ISM beyond the Local Bubble, and challenges in modeling the heliospheric/ISM interface.

New data and more sophisticated theoretical models with predictive power raised new questions and identified those areas where new observations, both remote sensing and *in* *situ* measurements, are needed. For example, the new data from Voyager 1's crossing of the termination shock at 94 AU (on December 16, 2004) and Voyager 2's crossing at 84 AU (on August 30, 2007, conveniently just before the workshop), provided critical data for use in new MHD models for inferring the orientation and strength of the interstellar magnetic field near the Sun.

To place these new data in context, one often needs new terminology, but it is critical not to confuse the nonexperts and even the experts. For example, what is the best name for the partially ionized plasma that surrounds the heliosphere — now that there is evidence that the heliosphere is located just outside of the Local Interstellar Cloud. After much discussion, the participants decided on the term "circum-heliospheric interstellar medium" or CHISM and proposed that this term be used in the future.

Looking to the near future, the participants hoped for the successful launch and operation of the Interstellar Boundary Explorer (IBEX) satellite and the repair of the high-resolution ultraviolet spectrometers on HST/STIS. They also looked forward to the analysis of both new and archival data for use with 3D kinetic MHD models of the solar wind interaction with the CHISM. The rapid increase in the power of modern computers should facilitate calculations with such complex models.

Looking further into the future, the participants saw the need for a fully instrumented space probe that would measure the plasma and magnetic-field properties through the termination shock and heliopause into the bow shock region and beyond into the CHISM, which is unaltered by the Sun's influence.

We conclude by thanking all of those who made this workshop an extraordinary success. We thank the Directors of ISSI for their generous sponsorship and, in particular, Ruedi von Steiger for his advice in planning and editorial matters. We also thank the local organization team led by Brigitte Fasler for its professional work in planning and supporting the workshop. We thank all of the workshop participants for their excellent presentations, insightful discussions, and well-written papers that constitute the legacy of the workshop. Finally, we thank our summary speaker for his excellent summary and insightful comments on all that transpired.

Dedication to Dr. George Gloeckler

Eberhard Möbius

Originally published in the journal Space Science Reviews, Volume 143, Nos 1–4, 5–6.
DOI: 10.1007/s11214-008-9476-3

The ISSI Workshop "From the Heliosphere to the Local Bubble" was dedicated to Dr. George Gloeckler on the occasion of his 70th birthday. This workshop, which has brought together space scientists and astrophysicists to talk about the galactic neighborhood of our solar system, could not have been better suited for this purpose.

Starting his career with the study of energetic particles from the Sun, George Gloeckler has contributed to this emerging field with roots in both scientific communities through visionary instrument development, effective team building and strategic placement, meticulous data analysis and innovative ways to extract previously inaccessible information. Recognizing that interplanetary space was full of energetic particles and that their generation and acceleration happened at lower energies, he pushed instrument development to new horizons, by injecting novel instrument designs into space physics. He was one of the first to realize the potential of time-of-flight mass spectrometers for particle populations from the solar wind to low energy cosmic rays.

This quest included the energy range of pickup ions that are implanted into the solar wind upon their ionization, thus acquiring between zero and four times the solar wind energy. After having built a time-of-flight spectrometer within the long-standing Maryland-Garching collaboration forged between George Gloeckler and Dieter Hovestadt, the author was fortunate to discover the first interstellar pickup ions. Being convinced of their universal importance, George Gloeckler exploited the capabilities of the Ulysses SWICS instrument, the concept and design of which he was responsible for, to land coup after coup in revealing parameters of the Sun's immediate neighborhood in the galaxy. Here are just a few key examples: He used the unique properties of He^{2+} pickup ions that had been predicted by the late Daniel Rucinski to derive the most precise interstellar He density, without the need of absolute sensor calibration. Together with Johannes Geiss, he extracted the cosmologically important $^3He/^4He$ ratio for the local interstellar gas from pickup ions. In the heliophysical

E. Möbius (✉)
Space Science Center and Department of Physics, University of New Hampshire,
Morse Hall, 8 College Road, Durham, NH 03824, USA
e-mail: Eberhard.Moebius@unh.edu

DOI: 10.1007/978-1-4419-0247-4_2

triumvirate with Johannes Geiss and Lennard Fisk, he derived the density of interstellar H in the heliosphere and subsequently constrained the ionization state of the interstellar medium and the strength of the surrounding magnetic field. They also demonstrated that pickup ions lend themselves much more easily to further acceleration than ions of the solar wind proper. At this Workshop, George Gloeckler surprised the audience once more with a very interesting new result. He showed how the ubiquitous suprathermal tails as seen by the Voyagers can be used to connect the well measured abundance ratios of several interstellar species with the precisely determined interstellar He density to deduce improved densities for these species.

An account of George Gloeckler's contributions to the scientific community and scientific advancement would be rather incomplete without noting his essential involvement in important committees, his foresight with the development of new methods, definition of new missions, and tireless politicking at agencies to get things into motion. Without his effort to repeatedly propose and push for a small and innovative mission to study the interstellar medium from within the inner heliosphere, the implementation of the Interstellar Boundary Explorer (IBEX) that has just been launched on October 19, 2008, would be unthinkable.

At this juncture, space exploration has reached the point when we truly start to venture into interstellar space and turn our attention to the connection with the wider neighborhood of our solar system. Therefore, it couldn't be more appropriate to connect the name of George Gloeckler with the topical ISSI Workshop that brought together scientists from space physics and astrophysics to start a serious collaboration. His contributions in the field have pointed into this direction for many years. Yet, this workshop has started such an endeavor in earnest.

Let me add a few personal notes. In the late 1970s and early 1980s when I had just switched from laboratory plasma to space physics, working with Dieter Hovestadt, visits to George Gloeckler's University of Maryland group were like coming to a buzzing hub in space science and a place where it felt like home. The group had attracted young scientists, such as Glenn Mason, Doug Hamilton, and Fred Ipavich, who flourished in this nurturing environment and subsequently established important programs of their own. This almost self-running success can be attributed in large part to George's inviting, friendly, and supportive personality, which makes it a pleasure to spend time with him also beyond professional encounters. There are fond memories of a hike in the Austrian Alps during a weekend of the COSPAR meeting in Innsbruck, which shaped ideas in my early career, and of a refreshing walk through Muir Woods, during which some of the concepts that ultimately led to IBEX were discussed. Finally, I must confess, George also had his helping hand in my career when he dropped my name at the Institute for the Study of Earth, Oceans, and Space of the University of New Hampshire. As a consequence, I was asked and then decided to cross the Atlantic. Joined by Lynn Kistler, one of Fred Ipavich's students, and later by Toni Galvin, one of George Gloeckler's own students, we often jokingly referred to our space plasma composition effort as "Maryland North".

At this point I would like to speak for all workshop participants and for the scientific community in our field in conveying our congratulations. We wish George many more years of fruitful scientific work and many more important results in this field whose golden age has just begun.

Section I: What Are the Three-Dimensional Shape and Structure Of The Dynamic Heliosphere?

The Solar Wind in the Outer Heliosphere

J.D. Richardson · E.C. Stone

Originally published in the journal Space Science Reviews, Volume 143, Nos 1–4, 7–20.
DOI: 10.1007/s11214-008-9443-z

Abstract The solar wind evolves as it moves outward due to interactions with both itself and with the circum-heliospheric interstellar medium. The speed is, on average, constant out to 30 AU, then starts a slow decrease due to the pickup of interstellar neutrals. These neutrals reduce the solar wind speed by about 20% before the termination shock (TS). The pickup ions heat the thermal plasma so that the solar wind temperature increases outside 20–30 AU. Solar cycle effects are important; the solar wind pressure changes by a factor of 2 over a solar cycle and the structure of the solar wind is modified by interplanetary coronal mass ejections (ICMEs) near solar maximum. The first direct evidences of the TS were the observations of streaming energetic particles by both Voyagers 1 and 2 beginning about 2 years before their respective TS crossings. The second evidence was a slowdown in solar wind speed commencing 80 days before Voyager 2 crossed the TS. The TS was a weak, quasi-perpendicular shock which transferred the solar wind flow energy mainly to the pickup ions. The heliosheath has large fluctuations in the plasma and magnetic field on time scales of minutes to days.

Keywords Solar wind · Termination shock · Heliosheath · Heliopause · Pickup ions · Interstellar neutral atoms · Anomalous cosmic rays

1 Introduction

We give a brief introduction to the solar wind in the outer heliosphere (HS) and discuss the interaction of the solar wind with the interstellar medium. Figure 1 shows an overview of the heliosphere, the bubble blown into the circum-heliospheric interstellar medium (CHISM) by

J.D. Richardson (✉)
Kavli Institute for Astrophysics and Space Research, Massachusetts Institute of Technology,
77 Massachusetts Avenue, Cambridge, MA 02139, USA
e-mail: jdr@space.mit.edu

E.C. Stone
Space Radiation Laboratory, California Institute of Technology, 1200 E. California Blvd., Pasadena,
CA 91125, USA

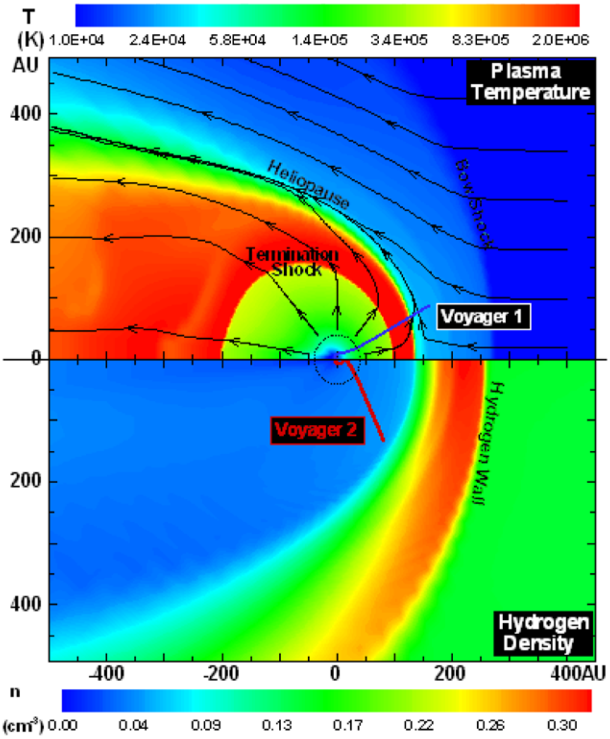

Fig. 1 A plot of the equatorial heliosphere from a plasma (*top*) and neutral (*bottom*) perspective. The *color bar* on the top panel shows the plasma temperature. The *lines* show the plasma flow. The main boundaries, the termination shock, heliopause, and bow shock are labeled. The *color bar* on the *bottom panel* shows the H density; the hydrogen wall in front of the heliopause is labeled and the trajectories of the Voyager spacecraft are shown. Figure courtesy of H. Müller

the solar wind which contains the Sun. Parker (1958) developed a theory for a supersonic solar wind at the dawn of the space age. His hypothesis was verified when the solar wind was first detected in the early 1960s (Gringauz 1961; Neugebauer and Snyder 1962).

The solar wind is seen in Fig. 1 flowing radially outward from the Sun. A corollary to Parker's theory is that the solar wind goes through a transition from supersonic to subsonic flow at the termination shock, where the solar wind senses the CHISM and deflects down the heliospheric tail (Weymann 1960). Figure 1 shows the CHISM moving to the left relative to the Sun. The size of the heliospheric bubble in the CHISM is determined by where the solar wind pressure is equal to the CHISM pressure (Parker 1963). The boundary between these two plasmas is called the heliopause (HP) and is analogous to the magnetopauses of Earth and other planets. The CHISM flow in this model is also supersonic (we don't know if the real CHISM is super- or sub-sonic), therefore it also goes through a shock so that the flow can divert around the heliosphere. The shock in the CHISM is called the bow shock. The region of shocked CHISM material which flows around the HS is called the outer heliosheath. The region of shocked solar wind where the solar wind diverts down the HS tail is called the inner heliosheath or commonly just the heliosheath.

The neutrals in the CHISM are not affected by the magnetic fields and flow into the heliosphere. Neutral He has few interactions with the plasma, so essentially pristine CHISM He flows into the inner HS where it can be directly measured by spacecraft (Witte 2004). The CHISM H interacts with the plasma both in the heliosheath (HSH) and in the solar wind via charge exchange. A proton gains an electron from a neutral; the neutral formed from the proton has a speed equal to the plasma speed. The newly created ion, called a pickup ion, is accelerated to the plasma speed and has an initial gyro-energy equal to the plasma flow

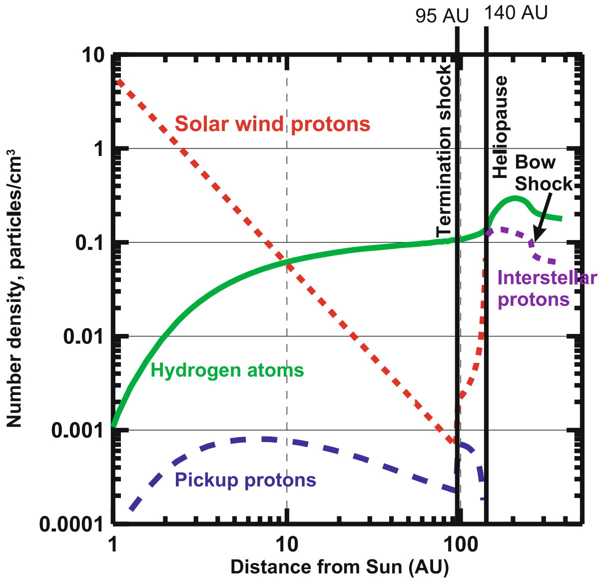

Fig. 2 The density of the plasma and neutral components from 1 to 1000 AU. The solar wind ions come from the Sun. The pickup ions are interstellar neutrals which have been ionized in the solar wind. The densities of the solar wind and of the pickup ions jump at the termination shock. Outside the heliopause, the ions are part of the CHISM. Both the ion and neutral density increase in front of the heliopause (in the hydrogen wall). The interstellar neutrals dominate the mass density outside 10 AU. Figure courtesy of V. Izmodenov

energy (about 1 keV in the solar wind). The energy for this acceleration comes from the plasma flow energy, so the plasma slows down (Richardson et al. 2008b).

One effect of charge exchange in the outer HSH is the formation of the hydrogen wall shown in Fig. 1. The CHISM plasma slows down as it approaches the heliopause. The CHISM H is coupled to this plasma via charge exchange, so it also slows down and thus has a higher density (Baranov and Malama 1993; Baranov and Malama 1995; Zank et al. 1996). This dense region upstream of the nose of the HS is called the hydrogen wall; similar walls are observed at other astrospheres (Linsky and Wood 1996).

Figure 2 shows the densities of ion and neutral populations in the heliosphere. The CHISM ion density increases at the bow shock where the flow speed decreases, but these ions do not enter the HS. The neutral density also increases at the bow shock, forming the hydrogen wall. The CHISM neutrals flow into the HS and are the HS population with the highest density outside 10 AU. The solar wind density decreases as R^{-2} out to the TS, increases at the TS, and again increases approaching the HP. The pickup ions, the ionized interstellar neutrals, make up an increasingly large fraction of the solar wind with distance and comprise about 20–30% of the solar wind at the TS (Richardson et al. 2008b). Since the pickup ions are hot, they dominate the thermal ion pressure outside 30 AU. Thus the CHISM not only stops the solar wind and diverts it down the tail, but also penetrates deep into the HS. This chapter discusses the outward flow of the solar wind and how it is affected by the CHISM.

2 Solar Wind Evolution

The slow solar wind reaches an asymptotic speed of about 400 km/s and, to first order, maintains that speed until the TS. Figure 3 shows 101-day averages of the solar wind speed, density, temperature and dynamic pressure at V2. The top panel also shows 101-day averages of the solar wind speed at 1 AU. Near the Sun (out to 30 AU) the speeds at Earth and

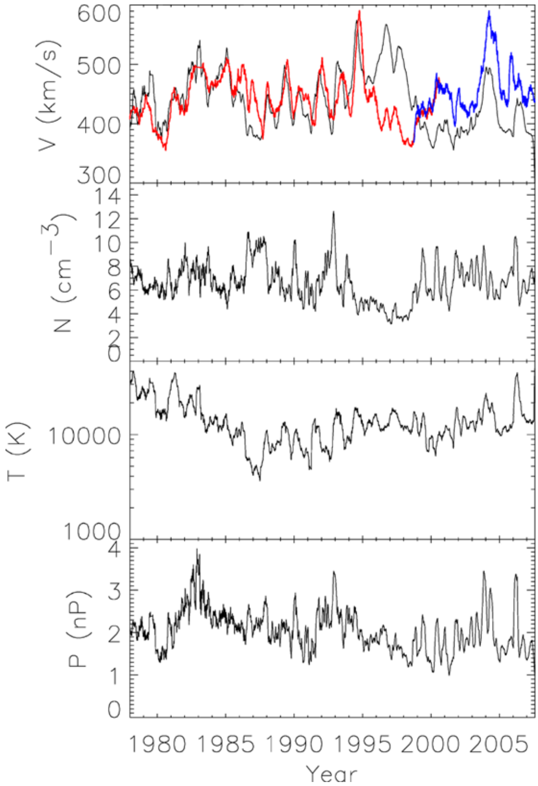

Fig. 3 Running 101-day averages of the solar wind speed, density, temperature and dynamic pressure observed by Voyager 2. The *top panel* also shows speeds at 1 AU from IMP 8 (*red*) and ACE (*blue*)

those at V2 are very similar. The solar wind parameters have a lot of variation, but to first order the speed is constant, the density decreases as R^2, and the temperature decreases out to 20–25 AU and then increases.

The solar wind changes over a solar cycle (Lazarus and McNutt 1990). The dynamic pressure, which determines the distance to the TS and HP, is least near solar maximum, increases for 2–3 years after solar maximum, then decreases to the next solar maximum (Richardson and Wang 1999). At solar maximum, the solar wind is slow and dense at all heliolatitudes. At solar minimum, the solar wind is slow and dense near the equator but fast and tenuous near the poles, with a transition region near 20–30° heliolatitude. This gradient in speed with heliolatitude at solar minimum causes the difference in solar wind speeds at Earth and V2 in 1986–87 and 1995–97. In 1986–87, V2 was at a lower average heliolatitude than Earth and observed lower speeds whereas from 1995–97 V2 was at a higher heliolatitude than Earth and observed much higher speeds. Variations also exist from solar cycle to solar cycle; the current solar minimum has a smaller solar wind dynamic pressure than in the previous two cycles (McComas et al. 2008). Other shorter scale features are also observed, such as the speed variations with a 1.3-year period observed from 1987–1998 (Richardson et al. 1995). This variation in speed was observed throughout the heliosphere and has been an occasional feature observed in historic solar wind data (Gazis et al. 1995; Szabo et al. 1995). A similar period has been observed in convection patterns in the Sun and may be related (Howe et al. 2000).

Solar activity varies over a solar cycle, with many more ICMEs at solar maximum than at solar minimum (Cane and Richardson 2003). As the ICMEs move outward, they expand until they reach 10–15 AU (Richardson et al. 2006); during solar maximum as much as 40% of the SW observed by V2 is from ICMEs. At times of high solar activity the Sun sometimes emits a series of ICMEs over time periods of days to months. The latter ICMEs catch up to earlier ICMEs and merge, compressing the solar wind ahead of them to form regions of high magnetic field and (often) density called merged interaction regions (MIRs) (Burlaga et al. 1984; Burlaga 1995; Richardson et al. 2002). Near solar maximum these structures dominate the solar wind profile; from 2001–2005 the MIRs observed in the outer solar system evolved so that the magnetic field, speed, density, and dynamic pressure were all correlated, resulting in large pressure pulses which reached the TS roughly twice each year and pushed it outward (Richardson et al. 2003).

3 Effects of the Neutral CHISM on the Solar Wind

The first effects of the CHISM on the solar wind are those of the neutral H and He which penetrate into the heliosphere. The solar wind contains stationary structures called pressure-balanced structures across which the pressure (thermal plus magnetic) is constant. By 20 AU, the observed structures could only be in balance if the plasma had a hot pickup ion component (Burlaga et al. 1994). The next observed effect of the CHISM neutrals was an increase in the thermal proton temperature starting between 20 and 30 AU, which overwhelmed the adiabatic cooling which would occur without a heat source. The pickup ions are the heat source; they are formed with a ring distribution (the particle trajectories are perpendicular to the field). These distributions are unstable and generate magnetic fluctuations which isotropize the distributions. The waves transfer a small amount (4%) of their to the thermal protons, which is enough to heat them as observed (Smith et al. 2006; Isenberg et al. 2005).

The slowdown of the solar wind due to pickup of CHISM neutrals increases with distance and was first reported near 30 AU (Richardson et al. 1995), although the slowdown was not observed in Pioneer 11 data at similar distances (Gazis 1995). By the time V2 neared the TS in 2007, the solar wind speed was about 83% of its speed at Earth, so the pickup ions made up about 19% of the total solar wind density (Richardson et al. 2008b). We note that the 17% decrease in speed represents a roughly 30% decrease in flow energy. Thus the neutrals from the interstellar medium acquire a substantial fraction of the solar wind energy well before the TS crossing.

4 The Termination Shock

The first direct sign of the approaching TS was a fairly sudden increase in tens of keV to MeV ions and electrons in mid-2002 observed at V1 but not at V2, which was 18 AU closer to the Sun (Krimigis et al. 2003; McDonald et al. 2003). Figure 4 shows that these ions streamed along the magnetic field lines in the outward direction, as if they were generated at the Sun. Although the approach of the TS seemed a likely source for these particles, the outward direction was initially confusing. An MIR passed V1 and V2 in early 2003, at which time the V1 particle fluxes decreased. The increased dynamic pressure associated with the MIR pushed the TS outward so the field lines at V1 became disconnected from the TS. The MeV particles were again observed starting in mid-2004, but the keV ions and electrons did not return until the start of 2004. This difference in particle energies suggests the connection to the TS was more distant, so that only the more energetic particles had time to make it to V1 before they were convected back to the TS with the solar wind flow.

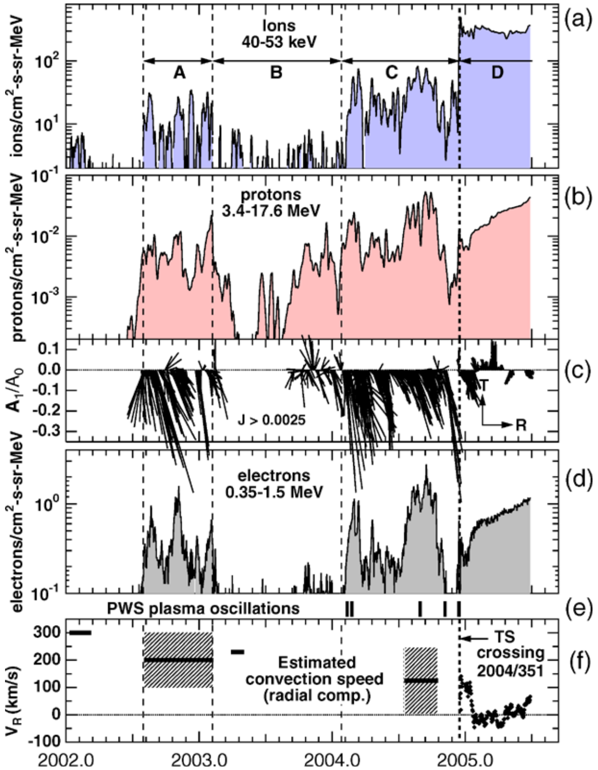

Fig. 4 Panels *1*, *2*, and *4* show 5-day smoothed V1 40–53 ion, 3.4–17.6 MeV proton, and 0.35–1.5 MeV electron intensities. Panel *3* shows the direction that particles are traveling. The *bottom panel* shows speeds estimated from the low-energy ions (since the plasma instrument is not working)

Another decrease, again likely due to an MIR, was observed in late 2004. Throughout this time period the particle intensities were highly variable and highly anisotropic (moving along the magnetic field away from the Sun). During a data gap on day 316, 2004, at 94 AU, V1 crossed the termination shock. The particle intensities jumped, became steady and isotropic, and the magnetic field magnitude increased (Burlaga et al. 2005; Decker et al. 2005; Stone et al. 2005).

The V1 TS crossing revealed the scale size of the heliosphere, roughly 90 AU for the TS and (based on models) 120–140 AU for the HP. Since V1 crossed the TS in a data gap, the TS strength (the ratio of downstream to upstream density and magnetic field, which is 4 for a strong shock) could only be estimated and was of order 2–3 (Burlaga et al. 2005; Stone et al. 2005). The HSH speeds derived from the particle data were very low just after the TS, −50 to 50 km/s (Decker et al. 2005), consistent with an inward-moving TS (Jokipii 2005). The keV particles seem to have their source at the TS, with a peak just outside the TS. However, the anomalous cosmic rays (ACRs), which were thought to be accelerated at the TS (Pesses et al. 1981), had intensities at the TS less than the peak values observed upstream in the solar wind and the flux of ACRs continued to increase after the TS crossing (Decker et al. 2005; Stone et al. 2005).

Let us return to the foreshock particles which were streaming the wrong way. They were telling us that the TS is blunt, with a larger radius of curvature than the Parker spiral field lines (Jokipii et al. 2004; Stone 2004). Figure 5 shows one such field line which has moved outward from the Sun. If the TS were blunt, the field line would first intersect the TS near where the TS is closest to the Sun, but would be in the solar wind on both sides. V1, as shown in the figure, would then see particles flowing from the TS in the direction outward

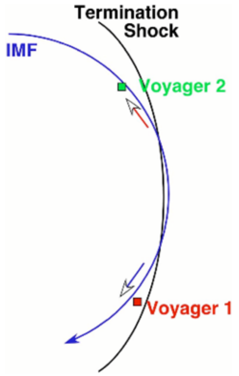

Fig. 5 Schematic diagram of a circular magnetic field line intersecting a blunt TS in two place. The Voyager spacecraft are on opposite sides of the nose of the heliosphere and see streaming in opposite directions as suggested by this figure

along the field line because this field line is connected to the TS. This hypothesis predicted that V2, on the other side of the closest point of the TS, would see particles streaming in the opposite direction. V2 entered the TS foreshock region in late 2004 and particles were streaming in the opposite sense (sunward) from those at V1, consistent with the blunt shock hypothesis (Decker et al. 2006).

V2 entered the foreshock region at 75 AU, about the same time V1 crossed the TS in late 2004. Since V1 entered this region at 85 AU, 10 AU further out, either the HS was asymmetric or the foreshock was much thicker in the V2 direction than the V1 direction. Models do suggest the foreshock is thicker at the V2 location because of the geometry of the crossing locations (Opher and Stone 2006), but only by a few AU. Models also show that, if the CHISM magnetic field were tilted from the CHISM flow direction, the heliosphere would be asymmetric (Linde et al. 1998; Ratkiewicz et al. 1998). Similar asymmetries are observed in Earth's magnetosphere (Paularena et al. 2001; Dmitriev et al. 2004) and in ICME models (Siscoe et al. 2007). The difficulty for global heliospheric models is to determine the actual CHISM field direction. Observations of a difference between flow directions of H and He coming into the HS provide constraints on this direction (Lallement et al. 2005; Izmodenov et al. 2005). Use of these field direction constraints in models gives HS asymmetries with the TS and HP closer in the south than the north, although the amount of the asymmetry varies between models (Opher et al. 2007; Pogorelov et al. 2007). V2 crossed the TS on day 242 of 2007 at 84 AU; calculations of the TS motion based on V2 solar wind data upstream of the TS and a 2-D model indicate the TS moved inward 2–3 AU between the V1 and V2 TS crossing, giving an asymmetry of 7–8 AU in the TS locations in the V1 and V2 directions (Burlaga et al. 2008; Decker et al. 2008; Richardson et al. 2008a; Stone et al. 2008).

Figure 6 shows daily averages of the plasma and magnetic field parameters before the TS crossing. The TS crossing is very obvious in the plasma data, marked by a sharp decrease in speed, an increase in temperature, and a change in flow angle. The density and magnetic field strength both increase, but these increases are comparable to increases observed in the solar wind. At the TS the solar wind begins to turn into a flow down the heliotail. The directions are as expected for this deflection, in the T and $-N$ directions (the RTN coordinate system has R radially outward, T parallel to the plane of the solar equator and positive in the direction of solar rotation, and N completes a right-handed system).

The solar wind begins to slow at about day 160, eighty days before the TS crossing, when a step-like decrease was observed. Two more downward speed steps were observed at days 190 and day 232, reducing the speed to near 300 km/s just before the TS. SW speeds of 300 km/s are sometimes observed near 1 AU, but V2 had not observed speeds this low since

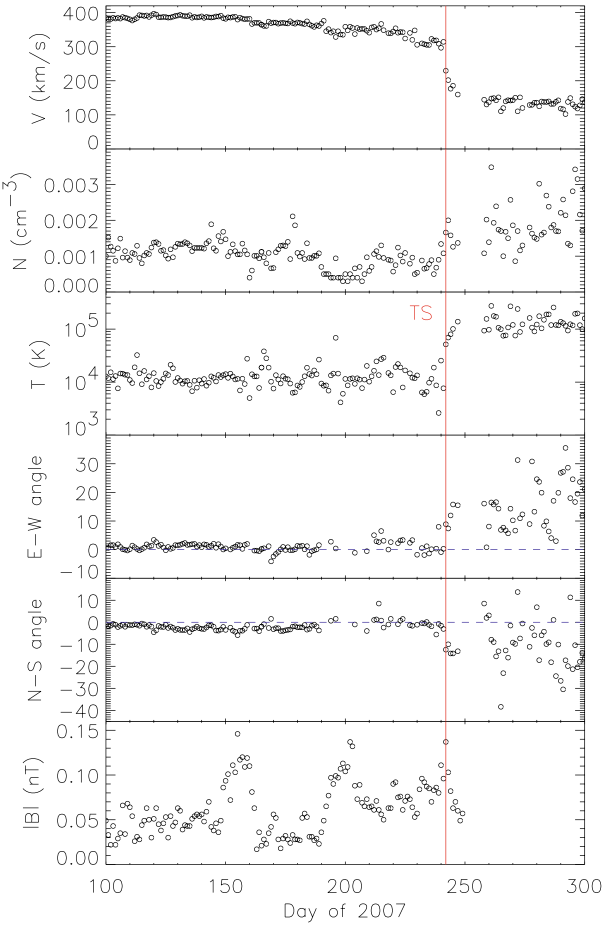

Fig. 6 Daily averages of the plasma speed, density, temperature, flow angles, and magnetic field magnitudes near the TS

1978, which suggests that these decreases are associated with the TS. The speed decrease from 380 to 300 km/s corresponds to a loss of about 40% of the solar wind flow energy before the TS. The first two speed decreases are associated with large increases in B. We do not yet understand the physics behind these speed decreases.

Figures 7 and 8 show the three crossings of the TS which occurred while V2 was being tracked. The first and fifth crossings occurred in data gaps. The third and fourth crossings at 244.0 and 244.11 have the classic foot ramp structure of a quasi-perpendicular, supercritical shock (Burlaga et al. 2008). At the foot, the magnetic field increases and the speed decreases; this region formed by ions which reflect from the shock. At the ramp the speed decreases and the temperature, density and field all increase. The second TS crossing at 243.84, a few hours earlier, looks very different. The speed steadily increases over about 30 minutes. The density does not have a clear increase but the temperature does jump. The magnetic field decreases across the foot region and two increases in the field were observed, both of which look like ramps. These data may show the TS in the process of reforming with the ramp moving upstream by an ion gyroradius (Burlaga et al. 2008).

Another surprise was the low thermal proton temperature in the heliosheath. Magnetosheaths of the outer planets all have proton temperatures of a few million degrees K and

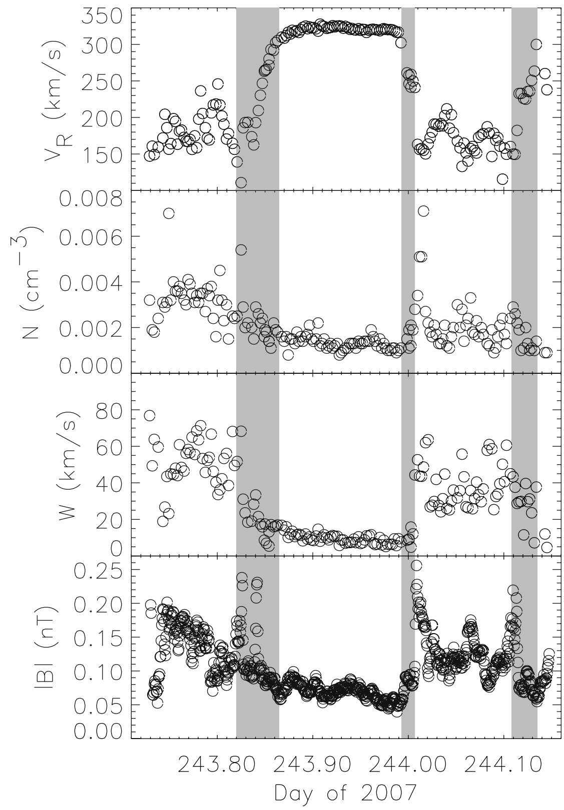

Fig. 7 The plasma speed, density, thermal speed, and magnetic field magnitudes near the TS

electron temperatures which are a factor of roughly 2 hotter. Models also predicted the HSH temperature would be a few million degrees. The models which predict these temperatures assume that almost all the SW flow energy goes into heating the thermal plasma, which is the case at the planetary magnetospheres. The observed HSH temperatures are about an order of magnitude less than these predictions, a few hundred thousand degrees K for protons (Richardson et al. 2008a). Electron temperatures are below the 10 eV instrument threshold; occasionally tails of the electron distributions are observed which allow us to estimate that the electron temperature is 3–4 hundred thousand degrees K.

What happens to the flow energy? We discussed above that about 40% of the flow energy is lost before the TS, probably heating energetic particles. The drop in speed at the TS is not a factor of 4 as at the planetary bow shocks but a factor of 2, so less energy is available for heating. But the major difference seems to be that most of the energy at the TS is going not to the thermal plasma but to the pickup ions. Based on V1 observations, Gloeckler et al. (2005) inferred that 80% of the flow energy transfered at the TS went into the pickup ions, which is consistent with the V2 plasma observations.

In addition to the average energy of the ions being low, some spectra look like they are not heated at all by the TS. Figure 9 shows examples of two ion spectra from the heliosheath which were fit to convected isotropic Maxwellian distributions. The first has a temperature of 22,000 K and the second a temperature of 228,000 K. The density and magnetic field go up by a factor of two at the shock, so the temperature should increase by a factor of two by conservation of the first adiabatic invariant. As shown in Fig. 9, some spectra in

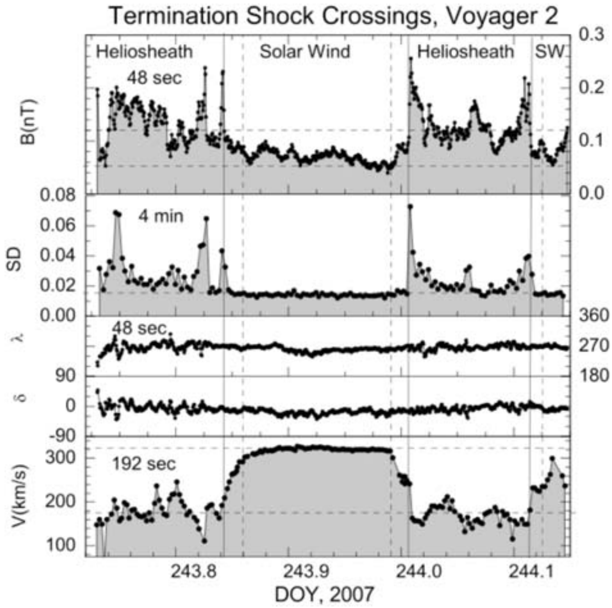

Fig. 8 The magnetic field magnitude, standard deviation of the magnetic field over 4-minute intervals, the azimuthal field angle, the elevations angle, and the plasma speed

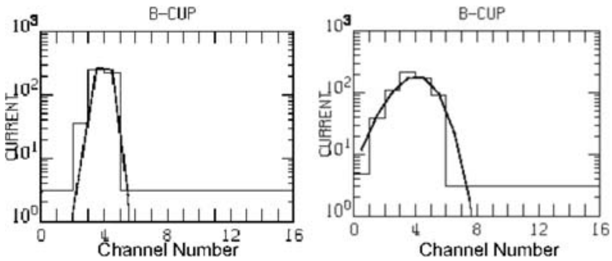

Fig. 9 Two-ion spectra from the heliosheath. Best fits of convected isotropic Maxwellian distributions to the histogram of observations of current versus energy are shown by the *curves*. For the *left* spectrum the temperature is 22,000 K and for the *right* spectrum it is 228,000 K

the HSH have temperatures of only 20,000 K, twice the average solar wind temperature. These protons were essentially unheated at the shock, they gained only the energy from compression of the plasma as it slowed at the shock. These cold spectra are seen sporadically throughout the heliosheath data encountered through August 2008. They could be plasma which has passed through the TS when it is in the process of reforming, or could have passed through the shock at a time when only hotter ions were effected by the shock (Zank et al. 1996). The TS is strongly time dependent based on the variations observed in the HSH.

Since data are available across the TS, the Rankine-Hugoniot equations can be solved to find the shock speed and normal (Richardson et al. 2008a). The shock normal angle is consistent with zero in the N direction but slightly off-radial in the T direction suggesting the shock has a smaller radius of curvature than a circle, opposite of the blunt shock hypothesized above. But this measurement is for one crossing of a very dynamic surface and so is not in real conflict with having a blunt TS. The TS was quasi-perpendicular and had compression ratios of 2.2–2.5 at TS-2 and 1.0–2.3 at TS-3. The shock moved at speeds of 50–100 km/s, similar to the speeds of planetary bow shocks. The upstream Mach numbers are 4.9 and 8.8 and the downstream Mach numbers are 1.1 and 2.8. These downstream Mach numbers highlight the lack of heating of the thermal plasma; this component of the plasma remains supersonic downstream of the TS. Thus the waves that convey information

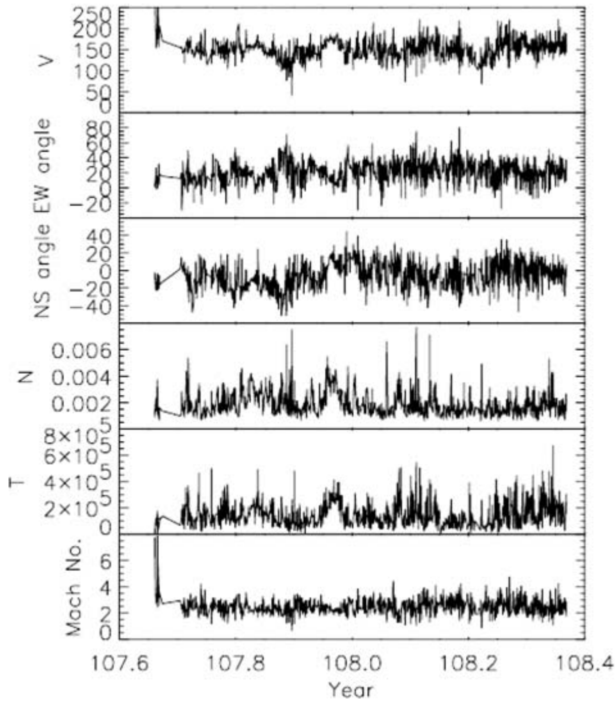

Fig. 10 The plasma speed, EW flow angle, NS flow angle, density, temperature,and Mach number of the thermal plasma

about the interstellar plasma upstream must propagate at speeds determined by the pickup ion sonic speed.

Figure 10 shows the plasma properties in the HSH. The average velocity components are 140 km/s in the radial direction, 47 km/s in the T direction, and -15 km/s in the $-N$ direction. The average speed is 144 km/s, density is 0.002 cm^{-3}, and $T = 144{,}000$ K. All the parameters are highly variable. These variations probably arise both from fluctuations in the shock speed, normal, and structure and from changes in the upstream solar wind. One feature which may be a solar wind feature is the increase in speed, density, and temperature beginning at about day 350 and lasting roughly 15 days. This increase is qualitatively similar to those observed in MIRs in the solar wind and is associated with a decrease in energetic particle fluxes, also analogous to a solar wind MIR. The N component of the speed changes from southward to northward at this time and remained northward for almost 40 days. This direction change suggests that a transient in the south pushed the flow ahead of it northward as it expanded.

5 Anomalous Cosmic Rays

Before the TS encounters, the TS was thought to be the source of anomalous cosmic rays (ACRs), singly ionized particles with energies of 20–100 MeV. These source of the ACRs are neutrals from the CHISM which are ionized, form pickup ions, and then are accelerated to high energy. The TS seemed a likely place for this acceleration to occur and pre-crossing expectations were that ACR intensities would peak at the TS and that the spectra would be power laws. The data from the TS in Fig. 4 shows that the low energy, tens of keV particle intensities peak at the TS but that the MeV particle intensities do not. Inspection of the particle spectra shows that the ACRs are modulated at the TS at both V1 and V2, so the ACRs are not accelerated where these spacecraft crossed the TS (Stone et al. 2005; Stone et al. 2008). Subsequent suggestions have been that the acceleration occurs in the flanks of the heliosphere (McComas and Schwadron 2008; Schwadron et al. 2008) or further out in the heliosheath (Fisk 2005).

6 Summary

The Voyager spacecraft are providing in situ observations of the interaction between the solar wind and the interstellar medium. The interstellar neutrals penetrate deep into the heliosphere and slow and heat the solar wind, removing about 35% of the solar wind energy before the TS. Upstream of the TS, a foreshock region of field-aligned streaming particles was observed. Ahead of the TS the solar wind slowed substantially starting 0.7 AU before the TS crossing. At the TS, little heating of the thermal plasma occurred with most of the energy going into the pickup ions. The HSH is a highly variable region due probably both to changes in the upstream solar wind and to motion of the TS.

Acknowledgements This work was supported by NASA; at MIT by NASA contract 959203 from JPL to MIT and NASA grant NAG5-8947.

References

V.B. Baranov, Y.G. Malama, Model of the solar wind interaction with the local interstellar medium–numerical solution of self-consistent problem. J. Geophys. Res. **98**, 15157–15163 (1993)

V.B. Baranov, Y.G. Malama, Effect of local interstellar medium hydrogen fractional ionization on the distant solar wind and interface region. J. Geophys. Res. **100**, 14755–14762 (1995)

L.F. Burlaga, F.B. McDonald, N.F. Ness, R. Schwenn, A.J. Lazarus, F. Mariani, Interplanetary flow systems associated with cosmic ray modulation in 1977–1980. J. Geophys. Res. **89**, 6579–6588 (1984)

L.F. Burlaga, N.F. Ness, J.W. Belcher, A. Szabo, P.A. Isenberg, M.A. Lee, Pickup protons and pressure-balanced structures: Voyager 2 observations in merged interaction regions near 35 AU. J. Geophys. Res. **99**, 21,511 (1994)

L.F. Burlaga, *Interplanetary Magnetohydrodynamics* (Oxford Univ. Press, London, 1995)

L.F. Burlaga, N.F. Ness, M.H. Acuna, R.P. Lepping, J.E.P. Connerney, E.C. Stone, F.B. McDonald, Crossing the termination shock into the heliosheath, magnetic fields. Science **309**, 2027–2029 (2005)

L.F. Burlaga, N.F. Ness, M.H. Acuna, R.P. Lepping, J.E.P. Connerney, J.D. Richardson, Observations of magnetic fields at the termination shock by Voyager 2. Nature **454**, 75–77 (2008)

H.V. Cane, I.G. Richardson, Interplanetary coronal mass ejections in the near-Earth solar wind during 1996–2002. J. Geophys. Res. **108**, 1156–1168 (2003). doi:10.1029/2002JA009817

R.B. Decker, S.M. Krimigis, E.C. Roelof, M.E. Hill, T.P. Armstrong, G. Gloeckler, D.C. Hamilton, L.J. Lanzerotti, Voyager 1 in the foreshock, termination shock, and heliosheath. Science **309**, 2020–2024 (2005). doi:10.1126/science.1117569

R.B. Decker, S.M. Krimigis, E.C. Roelof, M.E. Hill, Low-energy ions near the termination shock. In *Physics of the Inner Heliosheath: Voyager Observations, Theory, and Future Prospects*, AIP Conference Proceedings, vol. 258 (2006), pp. 73–78

R.B. Decker et al., Shock that terminates the solar wind is mediated by non-thermal ions. Nature **454**, 67–70 (2008)

A.V. Dmitriev, A.V. Suvorova, J.K. Chao, Y.-H. Yang, Dawn-dusk asymmetry of geosynchronous magnetopause crossings. J. Geophys. Res. **109**, A05203 (2004)

L.A. Fisk, Journey into the unknown beyond. Science **309**, 2016–2017 (2005)

P.R. Gazis, Limits on deceleration and asymmetry of solar wind speed. Geophys. Res. Lett. **22**, 2441–2444 (1995)

P.R. Gazis, J.D. Richardson, K.I. Paularena, Long term periodicity in solar wind velocity during the last three solar cycles. Geophys. Res. Lett. **22**, 1165–1168 (1995)

G. Gloeckler, L.A. Fisk, L.J. Lanzerotti, Acceleration of solar wind and pickup ions by shocks, in *Solar Wind 11/SOHO 16 Programme and Abstract Book (pdf file)*, European Space Agency (2005), p. 52
K.I. Gringauz, Some results of experiments in interplanetary space by means of charged particle traps on Soviet space probes. Space Res. **2**, 539–553 (1961)
R. Howe, J. Christensen-Dalsgaard, F. Hill, R.W. Komm, R.M. Larsen, J. Schou, M.J. Thompson, J. Toomre, Dynamic variations at the base of the solar convection zone. Science **287**, 2456–2460 (2000)
P.A. Isenberg, C.W. Smith, W.H. Matthaeus, J.D. Richardson, Turbulent heating of the distant solar wind by interstellar pickup protons with a variable solar wind speed, in *Proceedings of Solar Wind 11: Connecting Sun and Heliosphere*, ed. by B. Fleck, T.H. Zurbuchen. ESA SP-592 (European Space Agency, The Netherlands, 2005), pp. 347–350
V.V. Izmodenov, Y.G. Malama, M. Ruderman, Solar cycle influence on the interaction of the solar wind with Local Interstellar Cloud. Astron. Astrophys. **429**, 1069–1080 (2005). doi:10.1051/004-6361:20041348
J.R. Jokipii, J. Giacalone, J. Kota, Transverse streaming anisotropies of charged particles accelerated at the solar wind termination shock. Astrophys. J. **611**, L141–L144 (2004)
J.R. Jokipii, The magnetic field structure in the heliosheath. Astrophys. J. **631**, L163–L165 (2005)
S.M. Krimigis, R.B. Decker, M.E. Hill, T.P. Armstrong, G. Gloeckler, D.C. Hamilton, L.J. Lanzerotti, E.C. Roelof, Voyager 1 exited the solar wind at a distance of 85 AU from the Sun. Nature **426**, 45–48 (2003). doi:10.1038/nature02068
R. Lallement, E. Quemerais, J.L. Bertaux, S. Ferron, D. Koutroumpa, R. Pellinen, Deflection of the interstellar neutral hydrogen flow across the heliospheric interface. Science **307**, 1447–1449 (2005). doi:10.1126/science.1107953
A.J. Lazarus, R.L. McNutt, Jr., Plasma observations in the distant heliosphere: A view from Voyager, in *Physics of the Outer Heliosphere*, ed. by S. Grzedzielski, D.E. Page (Pergamon, New York, 1990), pp. 229–234
T.J. Linde, T.I. Gombosi, P.L. Roe, K.G. Powell, D.L. DeZeeuw, Heliosphere in the magnetized local interstellar medium: Results of a three-dimensional MHD simulation. J. Geophys. Res. **103**, 1889–1904 (1998)
J.L. Linsky, B.E. Wood, The Alpha Centauri line of sight: D/H ratio, physical properties of local interstellar gas, and measurement of heated hydrogen (the 'hydrogen wall') near the heliopause. Astrophys. J. **463**, 254–270 (1996)
D.J. McComas, N.A. Schwadron, An explanation of the Voyager paradox: particle acceleration at a blunt termination shock. Geophys. Res. Lett. **33**, L04102 (2006). doi:10.1029/2005GL025437
D.J. McComas et al., Weaker solar wind from the polar coronal holes and the whole Sun. Geophys. Res. Lett. **35**, L18103 (2008)
F.B. McDonald et al., Enhancements of energetic particles near the heliospheric termination shock. Nature **426**, 48–51 (2003)
M. Neugebauer, C.W. Snyder, Mariner 2 observations of the solar wind, 1, average properties. J. Geophys. Res. **71**, 4469–4484 (1962)
M. Opher, E.C. Stone, P.C. Liewer, The effects of a local interstellar magnetic field on Voyager 1 and 2 observations. Astrophys. J. **640**, L71–L74 (2006)
M. Opher, E.C. Stone, T.I. Gombosi, The orientation of the local interstellar magnetic field. Science **316**, 875–878 (2007). doi:10.1126/science.1139480
E.N. Parker, Dynamics of the interplanetary gas and magnetic fields. Astrophys. J. **128**, 664–676 (1958)
E.N. Parker, *Interplanetary Dynamical Processes* (Interscience, New York, 1963)
K.I. Paularena, J.D. Richardson, M.A. Kolpak, C.R. Jackson, G.L. Siscoe, A dawn-dusk density asymmetry in Earth's magnetosheath. J. Geophys. Res. **106**, 25377–25394 (2001)
M.E. Pesses, J.R. Jokipii, D. Eichler, Cosmic ray drift, shock wave acceleration, and the anomalous component of cosmic rays. Astrophys. J. **246**, L85 (1981)
N.V. Pogorelov, E.C. Stone, V. Florinski, G.P. Zank, Termination shock asymmetries as seen by the Voyager spacecraft: The role of the interstellar magnetic field and neutral hydrogen. Astrophys. J. **668**, 624 (2007)
R. Ratkiewicz, A. Barnes, G.A. Molvik, J.R. Spreiter, S.S. Stahara, M. Vinokur, S. Venkateswaran, Effect of varying strength and orientation of local interstellar magnetic field on configuration of exterior heliosphere: 3D MHD simulations. Astron. Astrophys. **335**, 363–369 (1998)
J.D. Richardson, C. Wang, The global nature of solar cycle variations of the solar wind dynamic pressure. Geophys. Res. Lett. **26**, 561–564 (1999)
J.D. Richardson, K.I. Paularena, A.J. Lazarus, J.W. Belcher, Evidence for a solar wind slowdown in the outer heliosphere? Geophys. Res. Lett. **22**, 1469–1472 (1995)
J.D. Richardson, K.I. Paularena, C. Wang, L.F. Burlaga, The life of a CME and the development of a MIR: From the Sun to 58 A. J. Geophys. Res. **106** (2002). doi:10.1029/2001JA000175

J.D. Richardson, C. Wang, L.F. Burlaga, Correlated solar wind speed, density, and magnetic field changes at Voyager 2. Geophys. Res. Lett. **30**, 2207–2210 (2003). doi:10.1029/2003GL018253
J.D. Richardson, Y. Liu, C. Wang, L.F. Burlaga, ICMES at very large distances. Adv. Space Res. **38**, 528–534 (2006)
J.D. Richardson, J.C. Kasper, C. Wang, J.W. Belcher, A.J. Lazarus, Termination shock decelerates upstream solar wind but heliosheath plasma is cool. Nature **454**, 63–66 (2008a)
J.D. Richardson, Y. Liu, C. Wang, D.J. McComas, Determining the LIC H density from the solar wind slowdown, Astron. Astrophys. (2008b, in press)
N.A. Schwadron, M.A. Lee, D.J. McComas, Diffusive acceleration at the blunt termination shock. Astrophys. J. **675**, 1584–1600 (2008)
G. Siscoe, P.J. MacNeice, D. Odstrcil, East–west asymmetry in coronal mass ejection geoeffectiveness. Space Weather **5**, S04002 (2007). doi:10.1029/2006SW000286
C.W. Smith, P.A. Isenberg, W.H. Matthaeus, J.D. Richardson, Turbulent heating of the solar wind by newborn interstellar pickup protons. Astrophys. J. **638**, 508–517 (2006)
E.C. Stone, A.C. Cummings, F.B. McDonald, B. Heikkila, N. Lal, W.R. Webber, Voyager 1 explores the termination shock region and the heliosheath beyond. Science **309**, 2017–2020 (2005)
E.C. Stone, Voyager in the vicinity of the termination shock: Observations and questions, Eos Trans. AGU, 85(47), Fall Meet. Suppl. (2004), Abstract SH41B-01
E.C. Stone et al., Voyager 2 finds an asymmetric termination shock and explores the heliosheath beyond. Nature **454**, 71–74 (2008)
A. Szabo, R. Lepping, J. King, Magnetic field observations of the 1.3-year solar wind oscillation. Geophys. Res. Lett. **22**, 1845–1848 (1995)
R. Weymann, Coronal evaporation as a possible mechanism for mass loss in red giants. Astrophys. J. **132**, 380 (1960)
M. Witte, Kinetic parameters of interstellar neutral helium—Review of results obtained during one solar cycle with the Ulysses/GAS-instrument. Astron. Astrophys. **426**(3), 835–844 (2004). doi:10.1051/0004-6361:20035956
G. Zank, H. Pauls, I. Cairns, G. Webb, Interstellar pickup ions and quasi-perpendicular shocks: Implications for the termination shock and interplanetary shocks. J. Geophys. Res. **101**, 457 (1996)

Constraints on the Structure of the Heliospheric Interface Based on Lyα Absorption Spectra

Brian E. Wood · Vladislav V. Izmodenov · Yury G. Malama

Originally published in the journal Space Science Reviews, Volume 143, Nos 1–4, 21–30.
DOI: 10.1007/s11214-008-9369-5

Abstract Spectroscopic observations of the hydrogen Lyα lines from nearby stars taken by the *Hubble Space Telescope* (HST) sometimes show absorption signatures from the heliosphere. This absorption is a unique diagnostic of material in the outermost parts of our heliosphere. We summarize how the HST data have been used to test various models of the heliosphere, particularly new 3-dimensional MHD models that have recently become available. We also focus on new detections of heliospheric absorption in very downwind directions, which can only be modeled using heliospheric model codes with extended grids in the downwind direction. We illustrate a couple attempts to reproduce this absorption using a couple of these extended tail models.

Keywords Solar wind · Interstellar medium · Heliosphere · Ultraviolet spectroscopy

1 Introduction

Ever since the first detection of Lyα absorption from the outer heliosphere in 1996 (Linsky and Wood 1996), the absorption has been used to test models of the heliosphere. The absorption comes from hot hydrogen that permeates the heliosphere due to charge exchange processes that occur during the collision of the solar wind and ISM. Detection of the absorption requires high resolution UV spectroscopy, and the only instruments capable of such observations are spectrometers on board the *Hubble Space Telescope* (HST); first the Goddard

B.E. Wood (✉)
JILA, University of Colorado, 440 UCB, Boulder, CO 80309-0440, USA
e-mail: woodb@colorado.edu

V.V. Izmodenov
Dept. of Aeromechanics and Gas Dynamics, Lomonosov Moscow State University, Moscow 119899, Russia
e-mail: izmod@ipmnet.ru

V.V. Izmodenov · Y.G. Malama
Space Research Institute (IKI), Russian Academy of Science, and Institute for Problems in Mechanics, Moscow 117526, Russia

High Resolution Spectrograph (GHRS) and then its 1997 replacement the Space Telescope Imaging Spectrograph (STIS), which unfortunately has been inoperable since August 2004.

The Lyα absorption has confirmed the existence of the "hydrogen wall" predicted by models to exist between the heliopause and bow shock (Baranov et al. 1991). Attempts have been made to use the absorption to constrain ISM properties around the Sun, but with limited success due to model dependence and the sensitivity of the absorption to too many ISM parameters (Wood et al. 2000, 2007a; Izmodenov et al. 2002). Finally, analogous astrospheric absorption detected in the HST spectra have been used to study the solar-like winds of nearby stars and determine how the properties of such winds vary with stellar age and activity (Wood et al. 2005a).

2 The Heliospheric Absorption Detections

Only a small fraction of the Lyα spectra of nearby stars in the HST archive show direct evidence of heliospheric absorption (Wood et al. 2005b). There are two primary factors that determine whether an observed line of sight will have a detectable heliospheric signal. One is the ISM hydrogen column density. Detecting heliospheric absorption requires that the absorption is separable from interstellar absorption. The higher the interstellar H column density, the broader the interstellar absorption, and the more likely that the ISM absorption will hide any heliospheric absorption.

The second factor is the direction of the line of sight with respect to the orientation of the heliosphere. This is quantified by the angle θ between the line of sight and the upwind direction of the ISM flow seen by the Sun, so $\theta = 0°$ is upwind and $\theta = 180°$ is downwind. Figure 1 plots the logarithmic interstellar H column density versus θ for all HST-observed lines of sight, with the boxes being lines of sight with detected heliospheric absorption and the diamonds being nondetections. As expected, the detections tend to have low ISM columns. It is also clearly easier to detect heliospheric absorption in upwind directions than in downwind directions. This is due to the stronger deceleration of heliospheric H in upwind directions, which helps to shift the heliospheric absorption away from the ISM absorption, making it easier to detect.

Most of the absorption detections are in directions where the hydrogen wall dominates the absorption, meaning the absorption is a diagnostic of neutral H properties in between

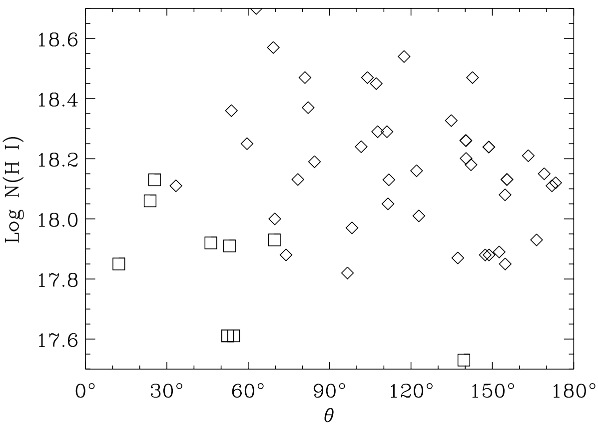

Fig. 1 The ISM H I column densities measured for all HST-observed lines of sight are plotted versus the angle of the lines of sight relative to the upwind direction of the ISM flow seen by the Sun. The *boxes* and *diamonds* indicate lines of sight that yield detections and nondetections of heliospheric absorption, respectively. From Wood et al. (2005b)

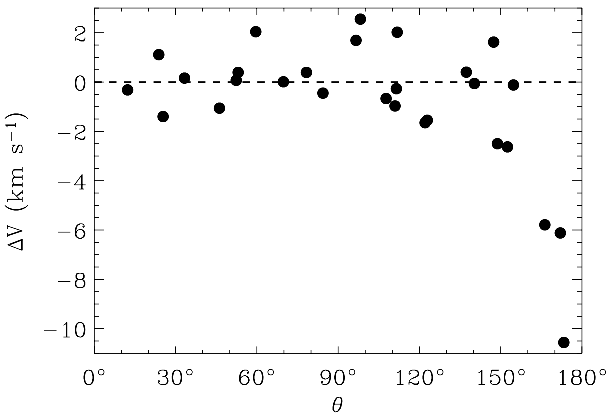

Fig. 2 Velocity difference between the bisectors of stellar Lyα lines and the stellar rest frame plotted as a function of θ, the angle between the line of sight and the ISM flow vector. The Lyα profiles of the most downwind lines of sight ($\theta > 160°$) are systematically blueshifted with respect to the stellar rest frame, suggesting the presence of heliosheath absorption. From Wood et al. (2007b)

the heliopause and bow shock. However, very downwind lines of sight with extended path lengths through the heliotail can potentially be dominated by absorption from heliosheath neutrals, neutrals formed by charge exchange in the inner heliosheath between the termination shock and heliopause. There is only one truly downwind heliospheric absorption detection in Fig. 1 where heliosheath absorption will dominate. The heliosheath absorption is much broader than the hydrogen wall absorption, but is also much shallower, which makes it harder to detect.

However, a less direct method of detecting heliosheath absorption has recently been devised (Wood et al. 2007b). The broad, shallow heliosheath absorption will absorb some of the flux from the red side of the observed stellar Lyα emission line. Therefore, the heliosheath absorption will cause the wings of the stellar emission line to be blueshifted relative to their original centroid, which would correspond to the stellar radial velocity. Figure 2 plots the velocity shifts of reconstructed stellar Lyα profiles as a function of θ. In most directions the profiles are within 2 km s^{-1} of the stellar radial velocity. But not in the most downwind directions with $\theta > 160°$. For the three lines of sight within 20° of the downwind direction the profiles are blueshifted relative to the star. This is the expected signature of broad heliosheath absorption, and the most downwind directions are where it is expected to be seen, so these three lines of sight can now be considered to represent heliospheric absorption detections, though the manner of detection is very different from the detections depicted in Fig. 1. The θ angle of 160° where the heliosheath absorption starts to become apparent may prove to be a useful diagnostic of the nature of the heliotail.

Figure 3 shows a sky map of the HST-observed lines of sight with Lyα spectra that have been searched for evidence of heliospheric absorption. The boxes are the lines of sight with detections of absorption, while the diamonds and plus signs are nondetections. As noted above, most of the detections are in the upwind direction, but the figure also shows the 3 new detections that are very close to the downwind direction. Even the nondetections can potentially be used to constrain models, as they place limits on the amount of heliospheric absorption that can be present in those directions. The 20 numbered lines of sight scattered around Fig. 3 indicate the sight lines that have been chosen in the past to test models (Wood et al. 2007a). These include the 11 sight lines with detected heliospheric absorption, and 9 sight lines with nondetections chosen to sample directions not covered by the detections.

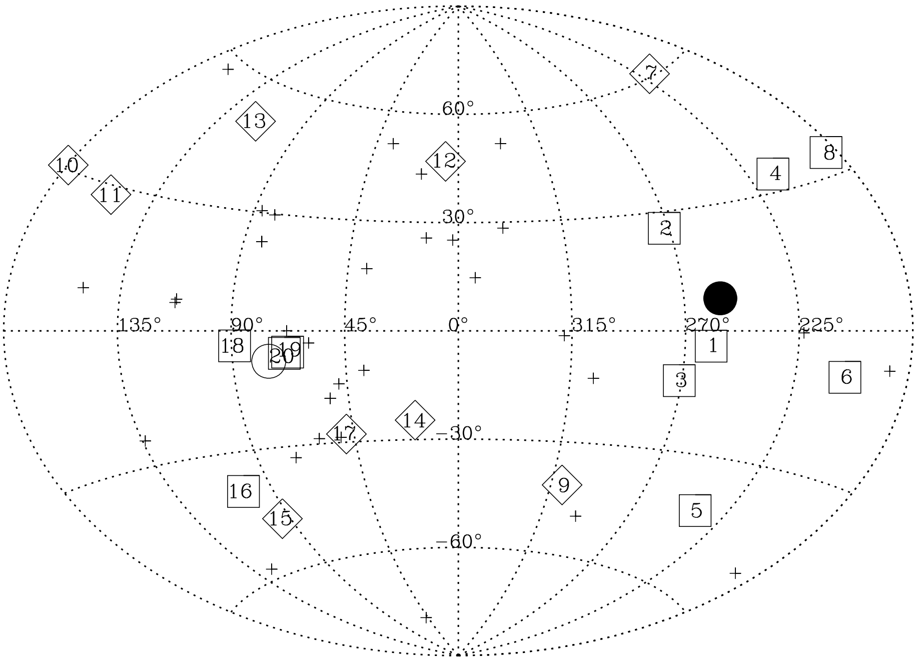

Fig. 3 Sky map in ecliptic coordinates of all HST-observed lines of sight with analyzed Lyα spectra. Numbered symbols indicate spectra that have been used to test model predictions of Lyα absorption (see Figs. 4, 5, and 7). *Boxes* indicate lines of sight with detected heliospheric absorption, while the *diamonds* and *plus signs* are nondetections. The *diamonds* indicate lines of sight with nondetections selected to provide upper limits for absorption in those directions. The *filled* and *open circles* indicate the upwind and downwind directions of the local ISM flow vector, respectively. From Wood et al. (2007a)

3 Absorption Dependence on the ISM Magnetic Field

Evidence for an asymmetric heliosphere has recently been provided by the *Voyager* satellites' observations near the termination shock, and by the different flow vectors measured for interstellar H and He within the solar system (Lallement et al. 2005; Opher et al. 2006; Stone and Richardson 2008). The principle cause of heliospheric asymmetry is expected to be an ISM magnetic field that is skewed with respect to the ISM flow seen by the Sun. The observations have stimulated the development of 3D MHD heliospheric models that can model the observed asymmetries and explore how heliospheric asymmetry depends on ISM field strength and orientation (Izmodenov et al. 2005; Opher et al. 2006; Pogorelov and Zank 2006; Opher et al. 2008; Izmodenov 2008). Some of these models are able to model the neutrals and can also be used to assess what effects the ISM magnetic field should have on the Lyα absorption diagnostic.

Figure 4 compares observed absorption with that predicted by models towards 4 of the lines of sight indicated in Fig. 2 (Wood et al. 2007a). The 3 models assumed different magnetic field strengths: $B = 0$, 1.25, and 2.5 μG. Field strengths higher than this tend to push the termination shock inside the 94 AU distance found by *Voyager 1* (Stone et al. 2005). The orientation of the magnetic field is assumed to be at an angle of $\alpha = 45°$ from the upwind direction of the ISM flow, in the plane suggested for the ISM field by the deflection of H atoms relative to He atoms within the solar system (Lallement et al. 2005). The

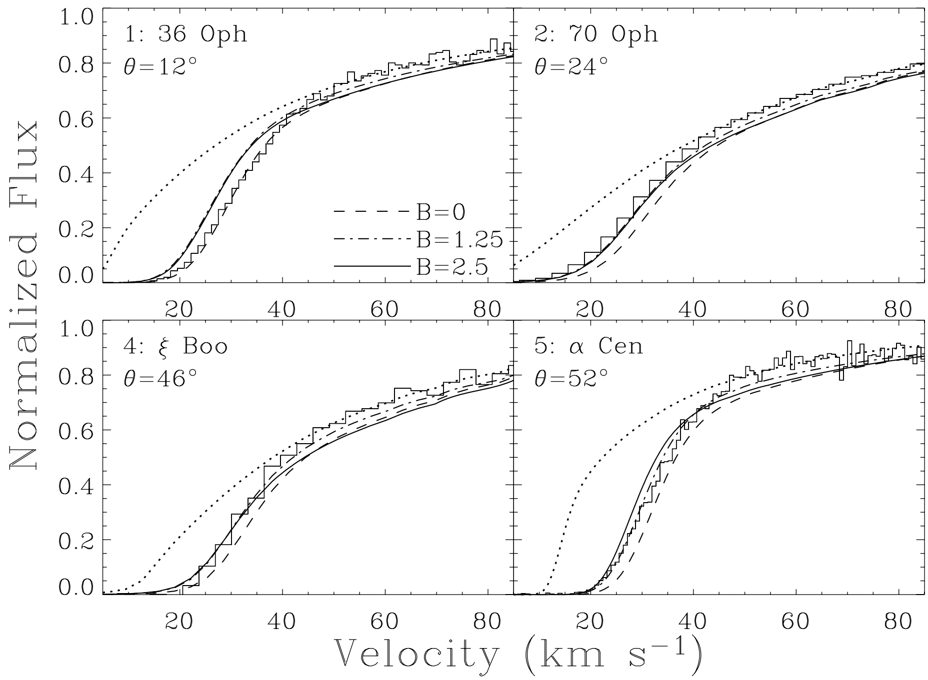

Fig. 4 The red side of the H I Lyα absorption line (histogram) for four stars with detection heliospheric absorption, with the number of the star indicating its location in Fig. 3. The stars are in order of increasing angle from the upwind direction of the ISM flow (θ). In each panel, the *dotted line* is the ISM absorption alone. Absorption predictions are shown for heliospheric models computed assuming ISM magnetic field strengths of 0, 1.25, and 2.5 μG (Wood et al. 2007a)

ISM hydrogen and proton densities assumed in these models are $n_\infty(\mathrm{HI}) = 0.18\ \mathrm{cm}^{-3}$ and $n_\infty(\mathrm{H}^+) = 0.06\ \mathrm{cm}^{-3}$, the ISM flow speed is $V_\infty = 26.4\ \mathrm{km\,s}^{-1}$, and the temperature is $T_\infty = 6400$ K (Izmodenov et al. 2005).

The panels in Fig. 4 show only the redshifted side of the Lyα absorption profiles where the heliospheric absorption will be located. Each panel shows the ISM absorption alone, and the excess absorption from the heliosphere, which the models are attempting to reproduce. Full descriptions of the Lyα data and its analysis can be found in Wood et al. (2005b).

Increasing the magnetic field generally decreases the amount of absorption, though there is little difference in the absorption predicted by the $B = 1.25$ μG and $B = 2.5$ μG models. The decrease is because a higher ISM field weakens the bow shock, leading to lower densities in the hydrogen wall and less absorption, despite the hydrogen wall being somewhat thicker (Wood et al. 2007a). The $B = 1.25$ μG and $B = 2.5$ μG models seem to fit the data particularly well in Fig. 4, though the $B = 0$ μG model works best for the most upwind line of sight (36 Oph). The lines of sight chosen in Fig. 4 are all upwind lines of sight with detected heliospheric absorption. There is little point in comparing the data and model predictions for downwind lines of sight because these particular models do not extend far enough downwind to capture all the absorption in such directions.

Not only does the absorption depend on the strength of the ISM field, it also depends on the orientation of the field. Figure 5 compares the observed absorption with that predicted by various models, for the same 4 lines of sight as in Fig. 4. The models are like the $B = 2.5$ μG model from Fig. 4, but with different α orientation angles. Rather than show the direct